A Circularly Polarized Patch Antenna Array with Reduced Mutual Coupling Using the Aperture-Loading Decoupling Technique

Xin Cheng, Bingyi Qian, Le Chang, Jinlin Liu, and Xiaoming Chen

School of Information and Communications Engineering
Xi'an Jiaotong University, Xi'an, 710049, China
changle@mail.xjtu.edu.cn

Abstract – An aperture-loaded decoupling strategy for 1×8 circularly polarized (CP) patch antenna array is presented in this article. By introducing an additional coupling path, the mutual coupling between adjacent antennas is cancelled. The result shows that more than 20-dB isolation enhancement is obtained by applying this strategy at the center frequency of 3.38 GHz. Mutual coupling between both adjacent and non-adjacent elements are suppressed to less than -25 dB. Moreover, the impedance bandwidth and axial ratio (AR) is also improved with decoupling. Compared with conventional CP antenna decoupling methods, the proposed approach has the characteristics of low profile, compact size, and low impact for the ground plane. It is shown that the AR bandwidth can be enhanced using the proposed decoupling method.

Index Terms – array antenna, circular polarization, decoupling aperture, mutual coupling reduction.

I. INTRODUCTION

In the past few years, attributed to the advantages of large system capacity and high spectral efficiency, 5G communication systems are universally applied in wireless communication systems. It is generally recognized that multiple-input multiple-output (MIMO) is a crucial technology for 5G wireless communications since it can significantly enhance channel capacity and spectrum efficiency [1, 2]. In a MIMO system, multiple antenna elements need to be packed in a restricted space, so that the separations between adjacent antennas are quite limited. However, mutual coupling effects between antenna elements severely deteriorates the performance of system. An inter-element spacing less than half a wavelength will make the influence of mutual coupling more devastating [3–5].

Recently, the suppression of mutual coupling in MIMO antenna arrays has attracted great interest in academia and industry. Typically, an in-band isolation of -17 dB is normally sufficient for small-scale MIMO

transmission [6–9]. Nevertheless, a lower mutual coupling level is critical since the efficiency of power amplifiers and active voltage standing wave ratio (VSWR) of array elements would also be influenced by mutual coupling in massive MIMO [3]. For instance, an active VSWR of the MIMO antennas would be higher than 6 at 15 dB isolation, and if the isolation is improved to more than 25 dB, the VSWR can be less than 2 [10–12]. Moreover, strong coupling in communication systems impacts radiation patterns of antenna elements and will cause nonlinear effects that decrease the amplifier efficiency [13, 14]. Therefore, the isolation level among massive MIMO elements is recommended to be better than 25 dB [15–17].

In the past decade, plentiful accomplishments have been published on the suppression of mutual coupling. For instance, Wu et al. proposed the concept of an antenna-array decoupling surface [12], which can introduce additional reflected electromagnetic waves to counteract the mutual coupling between adjacent elements. A similar technique is the decoupling ground [18]. Decoupling dielectric stubs can reduce mutual coupling of dual-polarized by localizing the electromagnetic field emitted by antenna elements, thus weakening the electromagnetic couplings to adjacent antenna elements [19]. Nevertheless, these methods inevitably increase the antenna profile.

Inserting dummy elements between antenna elements is a prevalent decoupling method. Chiu et al. proposed defective ground structures (DGS) to improve the isolation between planar inverted F antennas, patches, and monopoles [20]. However, conventional DGSs break the ground plane, increasing backward radiation. Besides, DGS is designed to be useful only for specific coupling situations. To improve the applicability of DGS design, Zhang et al. proposed a novel pixelated surface ground structure which can be utilized to various antenna designs [21]. Yang et al. introduced electromagnetic bandgap (EBG) structures between two patch antennas as a band-stop filter to reduce mutual coupling by 8 dB [22]. Yu et al. proposed a 3-D meta-material structure

(3DMMS), which prevents surface wave propagation through negative permeability and achieves isolation enhancement of more than 18 dB [23]. Nevertheless, EBG structures require large areas and therefore cannot be applied to compact arrays. Apropos of 3DMMS, its decoupling bandwidth is relatively limited. Neutralization lines (NL), counteracting the original coupling wave by introducing an extra coupling path, is an efficient method for decoupling dual-element antenna systems [24]. In [25], Luo et al. reported a MIMO antenna array with both metamaterial and neutralization line technology, which achieves gain and isolation enhancement of about 3dB and 30dB respectively. Otherwise, sparse MIMO arrays designed with the strategy of uniform linear array fitting principles can mitigate the mutual coupling [26]. Unfortunately, their complexity increases drastically for large antenna arrays.

More applicable for microstrip antenna than above works, adding a decoupling structure at feeding layer has preferences of low profile and small impact on antennas' radiation performance. For closely coupled binary arrays, lumped decoupling technologies have been investigated in detail in [7] and [27]. However, LC components may introduce parasitic effects, reducing the radiation efficiency. Alternatively, transmission line-based decoupling methods are more attractive. For instance, Cheng et al. designed a microstrip line-based decoupling network for two strongly coupled, asymmetric and unmatched antenna elements [8], where an analytical design formula has been provided. Decoupling networks for patch antenna arrays with single linear polarization were fabricated in [28] and [29]. Zhang et al. first applied the transmission line-based decoupling network to dual-polarized MIMO antenna arrays, eliminating mutual coupling between the vertical, horizontal, and diagonal pairs of elements without degrading the isolation of cross-polarized ports [10]. Furthermore, a decoupling method with filtering response based on T-shaped transmission line is applied to 4×4 patch antenna array [30]. Despite that the isolations in these designs are higher than 30 dB, their network configurations are complex. Recently, a novel aperture loading decoupling concept has been reported in [31]. By introducing an additional coupling path between adjacent elements through the feeding line and coupling aperture, the mutual coupling between two adjacent antennas can be reduced to less than -25 dB. Since no additional impedance matching network is required, this method is more convenient for large-scale dual polarization microstrip antennas.

Circularly polarized (CP) antennas are widely applied in navigation and communication systems due to their superior ability to suppress multipath fading and polarization mismatch. However, studies on reducing coupling between large-scale circularly polarized microstrip antennas are quite rare [32–34]. In general, decoupling of CP arrays are more difficult than that for dual-linear-polarized arrays because the former require both linearly polarized components to be equally suppressed by the decoupling technique [33].

In this paper, we apply the aperture-loaded decoupling concept to CP array antennas. By etching small apertures at the ground plane, the feeding line of an element can generate additional coupling path with its adjacent antenna element through an aperture. With appropriate dimensions, these coupling apertures will cancel out the original coupling. Compared with existing decoupling methods of CP microstrip antennas, the proposed scheme features simple structure, higher decoupling efficiency, and low profile.

II. ANALYSIS OF THE CIRCULARLY POLARIZED DECOUPLING STRATEGY

In this section, the principle of decoupling approach is illustrated analytically. Figure 1 indicates the proposed CP patch antennas decoupling method, which consists of three identical elements, labelled as Antennas 1, 2, and 3. The operating frequency of patch antennas in this work is 3.38 GHz. The centre distance between adjacent patches is $0.5 \lambda_0$, where λ_0 is the free-space wavelength at the centre frequency. In particular, a chamfer length Lc provides two slightly separated resonant frequencies to achieve circular polarization with single-feed structure. Below the edge of each antenna element, two coupling apertures are etched into the ground layer. For comprehensive consideration, we take Antenna 2 as the reference antenna for analysis. The feeding line of Antenna 2 passes through the apertures loaded under Antennas 1 and 3 successively, generating extra coupling paths with
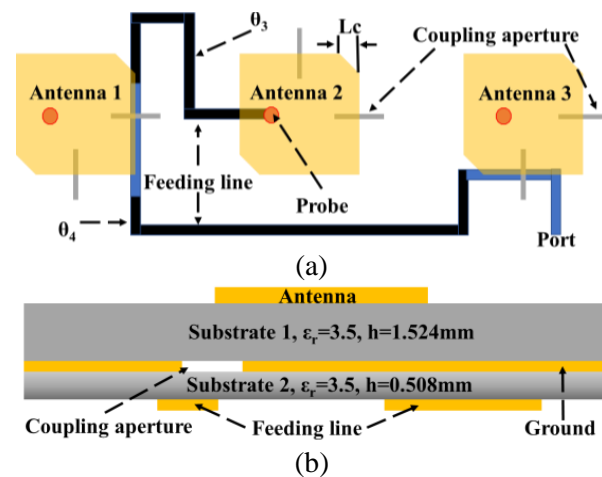

Fig. 1. Geometries of the proposed CP patch antennas decoupling method. (a) Top view. (b) Lateral view. (Lc=2.4mm, θ_3=470° and θ_4=860°.)

its adjacent antennas. By adjusting the size of the coupling aperture, the level of the new coupling path between two antennas can be optimized. When those two couplings have similar magnitudes and opposite phases, high isolation can be achieved.
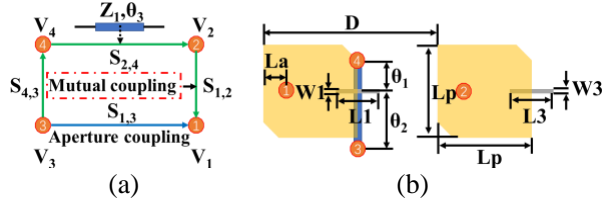

Fig. 2. Configuration of the decoupling between Antennas 1 and 2. (a) Signal flow diagram. (b) Simplified four-port model. (θ_1=45°, θ_2=90°, and La = 6.8 mm, L1=4.6 mm, L3=4 mm, W1=W3=0.2 mm, Lp=22.7 mm.)

For single-feed CP antenna, each element needs to be decoupled from the adjacent antennas on the right and left sides through a single microstrip line. Subsequently, the decoupling process of the CP array can be divided into two similar and related steps, as shown in Figs. 2 and 3. The signal flow diagram for the decoupling between Antennas 1 and 2 is shown in Fig. 2 (a), where two different coupling paths are indicated by green and blue arrows, respectively. The corresponding simplified four-port model is given in Fig. 2 (b). Define V_3 as the input voltage of Node 3. At Node 1, the output voltage is determined by these two paths, which can be written separately as:

$$V_{1,B} = S_{1,3}V_3, \tag{1.a}$$

$$V_{1,G} = S_{4,3}S_{2,4}S_{1,2}V_3, \tag{1.b}$$

where $S_{1,3}$ indicates the coupling through the loaded aperture, while the mutual coupling between radiation elements is denoted as $S_{1,2}$. According to transmission line theory,

$$S_{2,4} = \frac{2Z_0Z_1}{2Z_0Z_1\cos\theta_3 + j(Z_0^2 + Z_1^2)\sin\theta_3}. \tag{2}$$

For Nodes 3 and 1, we can write the decoupling condition as:

$$V_1 = V_{1,G} + V_{1,B} = 0. \tag{3}$$

Combining (1)-(3), the design condition can be obtained as follows:

$$S_{1,3} + \frac{2Z_0Z_1S_{4,3}S_{1,2}}{2Z_0Z_1\cos\theta_3 + j(Z_0^2 + Z_1^2)\sin\theta_3} = 0. \tag{4}$$

As for $S_{4,3}$, $S_{1,3}$ and $S_{1,2}$, it can be conveniently obtained through full-wave simulations. Meanwhile, the impedance matching from Node 3 to Node 2 should also be properly considered.

Figure 3 (a) illustrates the decoupling signal flow diagram of Antennas 2 and 3, with the condition that An-

tennas 1 and 2 are already decoupled. The corresponding simplified model is given in Fig. 3 (b). By repeating the above derivation and analysis, the value of θ_4 and the aperture parameters can be determined. Attributed to non-centrosymmetric antenna elements, the decoupling parameters of odd-positioned elements are different to those of even-positioned. A four-element array decoupled by the proposed method is depicted in Fig. 3 (c). After that, the xoz and yoz planes of each radiating element are decoupled with the xoz and yoz planes of its adjacent elements, respectively. This indicates that after decoupling, when a port is excited, its adjacent radiation patch apertures are in the voltage null. The area around the adjacent antenna elements can be considered as the quasi-voltage-zero region, thus suppressing the electromagnetic propagation. For ease of analysis, the characteristic impedance of all the transmission lines is chosen to be 50 Ω.
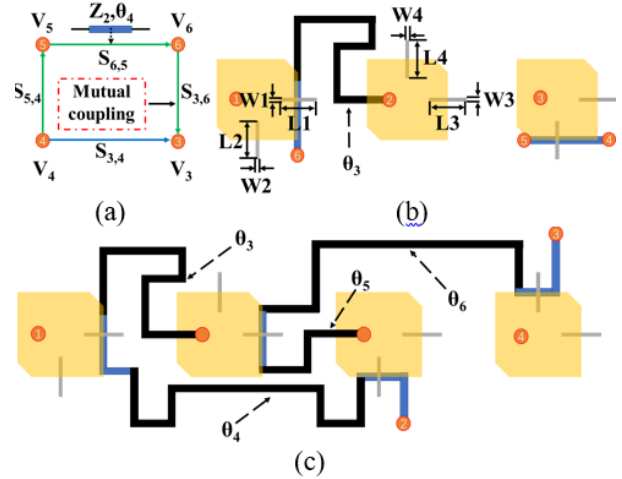

Fig. 3. Decoupling configuration of multiple antenna elements. (a) Signal flow diagram of the decoupling between Antennas 2 and 3. (b) Simplified six-port model. (c) Configuration of a four-element array with the proposed decoupling method. (θ_5=258.3°, θ_6=662.2°, and L2=4 mm, L4=4.8 mm, W2=W4=0.2 mm.)

III. MEASUREMENT RESULTS AND DISCUSSION

To demonstrate the decoupling performance of the proposed prototype, an 8-element CP microstrip antenna array was fabricated and measured, as shown in Fig. 4. Both the ground plane, microstrip patch and feeding line are printed on F4B with a loss tangent of 0.002 and a dielectric constant of 3.5. The array antenna is fixed with some screws, of which metal screws are used at the outmost sides and nylon screws are used for the parts close to the patch. All screws have been taken into account during electromagnetic simulations. The overall

size of this antenna array is 440×90 mm^2. The radiation performance and S-parameters of the proposed array are measured.
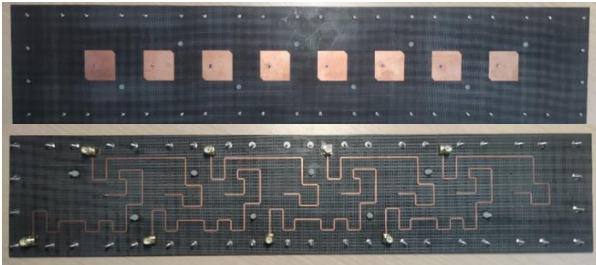

Fig. 4. Photograph of the fabricated 1×8 antenna array.
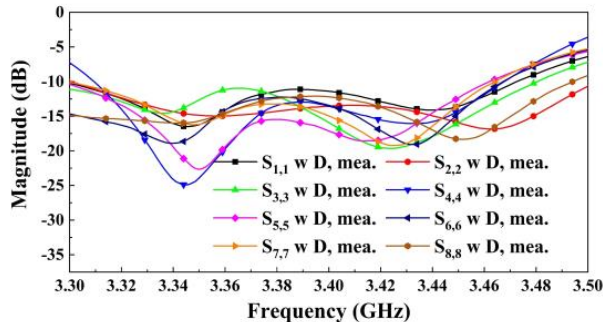

Fig. 5. Measured scattering parameters of the fabricated 1×8 array.

The measured reflection coefficients of the fabricated patch antenna array are depicted in Fig. 5. One can immediately see that the reflection coefficients of the 8 ports are better than -10 dB in the frequency range of 3.31-3.45 GHz. The reflection coefficients and ports isolations of some representative ports are plotted in Fig. 6. It demonstrates that the maximum mutual coupling level occurs between adjacent ports, and ports isolation are remarkably enhanced after decoupling, increasing from 18.7 dB to more than 30 dB at around 3.38 GHz (where the axial ratio is below than 3 dB). It is worth mentioning that the measured impedance bandwidth is wider than the simulated one. This may be caused by air gaps due to assembly tolerances and non-ideal contacts.

Figure 7 depicts the comparison of axial ratio (AR) of the CP antenna array with and without decoupling of Ports 1-4. It is observed that the AR of all ports improves after decoupling. A 3-dB AR bandwidth from 3.36 to 3.4 GHz is achieved for all four ports, which is slightly better than the simulation one. It suggests that the antenna array has excellent CP characteristics, and the reduction of coupling can significantly improve the AR of the patch antenna elements.
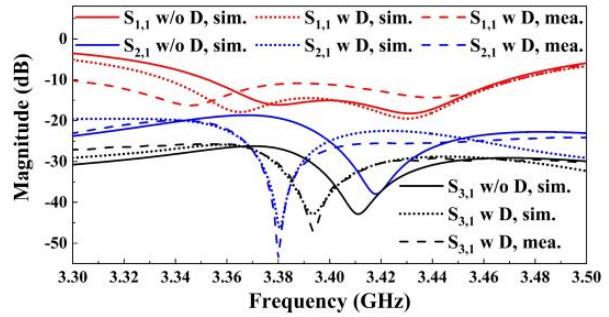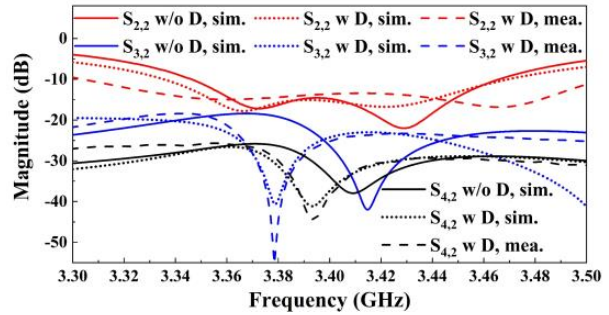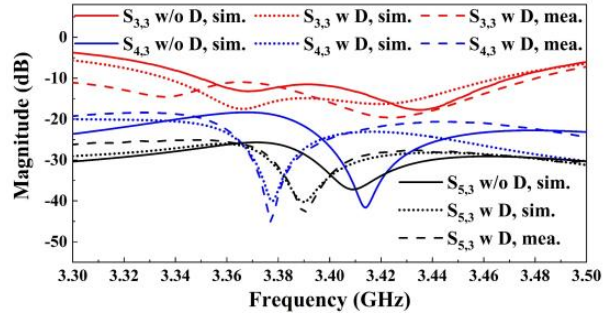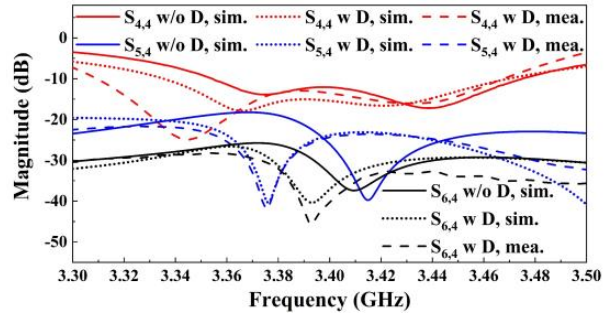

Fig. 6. Measured and simulated S-parameters of representative ports. (a) Port 1. (b) Port 2. (c) Port 3. (d) Port 4.

Figure 8 plots the simulated and measured radiation patterns of LHCP and RHCP of Ports 2-4 at 3.38 GHz with and without decoupling. It can be found that the radiation patterns of three elements are almost the same as the ones before decoupling. This
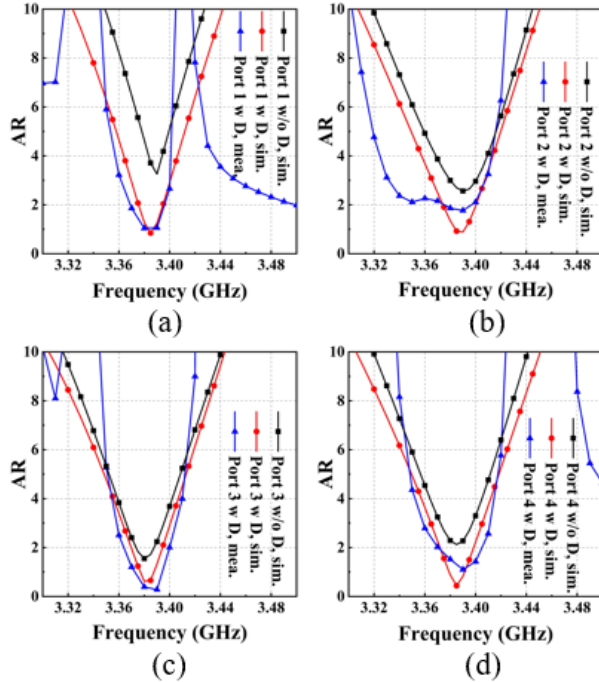
Fig. 7. Measured and simulated AR of representative ports. (a) Port 1. (b) Port 2. (c) Port 3. (d) Port 4.
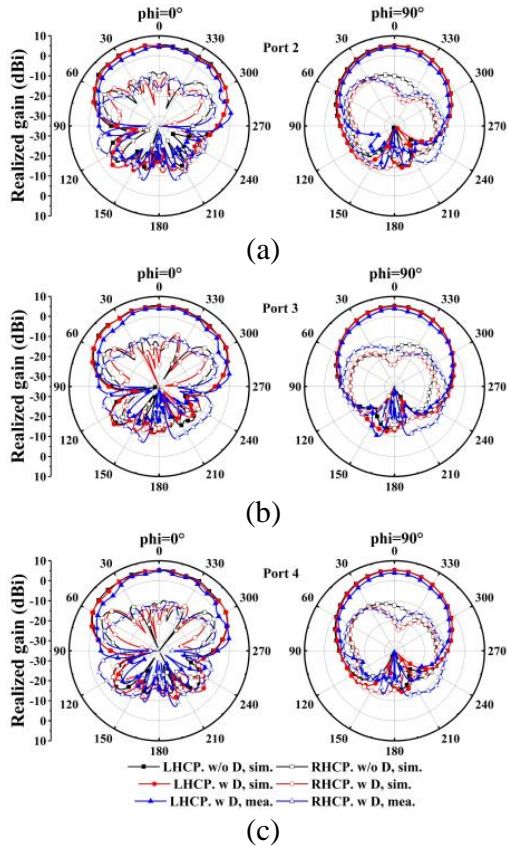

Fig. 8. Measured and simulated radiation patterns of representative ports. (a) Port 2. (b) Port 3. (c) Port 4.

demonstrates that the proposed decoupling strategy has faint effect on the radiation patterns of array antenna. As for the measurement results, they are marginally deteriorating than the simulation results. The discrepancy is mainly caused by measurement error and manufacturing tolerance.

Table 1: Performance comparison with published decoupling methods

Ref.	No. of Antennas	Polarization	Isolation	Profile
[10]	16	Dual-linear	$\geq$25 dB	0.09 λ_0
[31]	16	Dual-linear	$\geq$25 dB	0.08 λ_0
[19]	16	Dual-linear	$\geq$25 dB	0.47 λ_0
[32]	4	Circular	$\geq$19 dB	0.09 λ_0
[34]	2	Circular	$\geq$50 dB	0.012 λ_0
This work	8	Circular	$\geq$25 dB	0.02 λ_0

A detailed comparison of recently published decoupling works for linearly polarized and circularly polarized patch antenna array is summarized in Table 1. We are concerned with the polarization mode, antenna profile, and isolation between two ports. Compared to [10], our proposed decoupling scheme is of low complexity and superior in design simplicity. The proposed decoupling methods in [10] and [19] are only validated for antenna arrays with dual-linear-polarizations. The mutual coupling between antennas in [32] does not decrease below -20 dB, thus its applications in massive MIMO are limited. Moreover, the profile of the proposed prototype in this work is only 0.02 λ_0, which is far less than those in [10, 19, 31, 32]. In [34], on account of appreciable damage to the ground plane, the backward radiation is deteriorated distinctly. The decoupling bandwidth of the antenna proposed in this work is comparable to its 3-dB AR bandwidth, which is usually small for single-feed CP antennas. In general, the presented decoupling strategy shows overall superiority to the previous works.

IV. CONCLUSION

CP antennas have been heavily employed in satellite communications and navigation systems, yet there are few papers about the decoupling of CP patch antennas. Focusing on the status quo, a compact and low-profile decoupling strategy to enhance the isolation within 1×8

CP microstrip antenna array has been proposed in this paper. An additional coupling path could be generated through a coupling aperture to counteract the mutual coupling, which considerably enhances the isolation between antenna elements. Furthermore, both impedance bandwidth and AR could be improved using the proposed scheme.

ACKNOWLEDGMENT

REFERENCES

[1] A. Zaidi, F. Athley, J. Medbo, U. Gustavsson, and G. Durisi, *5G Physical Layer: Principles, Models and Technology Components*, Academic Press, London, U.K., 2018.

[2] H. Pei, X. Chen, X. Huang, X. Liu, X. Zhang, and Y. Huang, "Key issues and algorithms of multiple-input-multiple-output over-the-air testing in the multi-probe anechoic chamber setup," *Sci. China: Inf. Sci.*, vol. 65, no. 3, 131302, Mar. 2022.

[3] X. Chen, S. Zhang, and Q. Li, "A review of mutual coupling in MIMO systems," *IEEE Access*, vol. 6, pp. 24706-24719, Apr. 2018.

[4] J. W. Wallace and M. A. Jensen, "Mutual coupling in MIMO wireless systems: A rigorous network theory analysis," *IEEE Trans. Wireless Commun.*, vol. 3, no. 4, pp. 1317-1325, Jul. 2004.

[5] Y. Da, X. Chen, and A. A. Kishk, "In-band mutual coupling suppression in dual-band shared-aperture base station arrays using dielectric block loading," *IEEE Trans. Antenna Propag.*, vol. 70, no. 10, pp. 9270-9281, Oct. 2022.

[6] K. Qian, L. Zhao, and K. Wu, "An LTCC coupled resonator decoupling network for two antennas," *IEEE Trans. Microw. Theory Techn.*, vol. 63, no. 10, pp. 3199-3207, Oct. 2015.

[7] H. Meng and K. Wu, "An LC decoupling network for two antennas working at low frequencies," *IEEE Trans. Microw. Theory Techn.*, vol. 65, no. 7, pp. 2321-2329, Jul. 2017.

[8] Y. Cheng and K. M. Cheng, "A novel dual-band decoupling and matching technique for asymmetric antenna arrays," *IEEE Trans. Microw. Theory Techn.*, vol. 66, no. 5, pp. 2080-2089, May 2018.

[9] B. Qian, X. Chen, and A. A. Kishk, "Decoupling of microstrip antennas with defected ground structure using the common/differential mode theory," *IEEE Antennas Wireless Propag. Lett.*, vol. 20, no. 5, pp. 828-832, May 2021.

[10] Y. Zhang, S. Zhang, J. Li, and G. F. Pedersen, "A transmission-line-based decoupling method for MIMO antenna arrays," *IEEE Trans. Antennas Propag.*, vol. 67, no. 5, pp. 3117-3131, May 2019.

[11] M. Li, X. Chen, A. Zhang, W. Fan, and A. A. Kishk, "Split-ring resonator-loaded baffles for decoupling of dual-polarized base station array," *IEEE Antennas Wireless Propag. Lett.*, vol. 19, no. 10, pp. 1828-1832, Oct. 2020.

[12] K. Wu, C. Wei, X. Mei, and Z. Zhang, "Array-antenna decoupling surface," *IEEE Trans. Antennas Propag.*, vol. 65, no. 12, pp. 6728-6738, Dec. 2017.

[13] C. Fager, X. Bland, K. Hausmair, J. C. Cahuana, and T. Eriksson, "Prediction of smart antenna transmitter characteristics using a new behavioral modeling approach," *IEEE MTT-S Int. Microw. Symp. Dig.*, Tampa, FL, USA, pp. 1-4, Jun. 2014.

[14] F. Peng, F. Yang, B. Liu, and X. Chen, "Experimental investigation of decoupling effect on the nonlinearity of power amplifiers in transmitter array," *Applied Computational Electromagnetics Society (ACES) Journal*, in press.

[15] B. Wang, Y. Chang, and Y. Sun, "Performance of the large-scale adaptive array antennas in the presence of mutual coupling," *IEEE Trans. Antennas Propag.*, vol. 64, no. 6, pp. 2236-2245, Jun. 2016.

[16] Y. Da, Z. Zhang, X. Chen, and A. A. Kishk, "Mutual coupling reduction with dielectric superstrate for base station arrays," *IEEE Antennas Wireless Propag. Lett.*, vol. 20, no. 5, pp. 843-847, May 2021.

[17] Y. Zhang, S. Zhang, J. Li, and G. F. Pedersen, "A wavetrap-based decoupling technique for 45° polarized MIMO antenna arrays," *IEEE Trans. Antennas Propag.*, vol. 68, no. 3, pp. 2148-2157, Mar. 2020.

[18] S. Song, Y. Da, B. Qian, X. Huang, X. Chen, Y. Li, and A. A. Kishk, "Dielectric resonator magnetoelectric dipole arrays with low cross polarization, backward radiation, and mutual coupling for MIMO base station applications," *China Communications*, in press.

[19] P. Mei, Y. Zhang, and S. Zhang, "Decoupling of a wideband dual-polarized large-scale antenna array with dielectric stubs," *IEEE Trans. Veh. Technol.*, vol. 70, no. 8, pp. 7363-7374, Aug. 2021.

[20] C. Chiu, C. Cheng, R. D. Murch, and C. R. Rowell, "Reduction of mutual coupling between closely-packed antenna elements," *IEEE Trans. Antennas Propag.*, vol. 55, no. 6, pp. 1732-1738, Jun. 2007.

[21] Y. Zhang, S. Shen, Z. Han, C. Chiu, and R. Murch, "Compact MIMO systems utilizing a pixelated surface: capacity maximization," *IEEE Trans. Veh. Technol.* vol. 70, no. 9, pp. 8453-8466, Sep. 2021.

[22] F. Yang and Y. Rahmat-Samii, "Microstrip antennas integrated with electromagnetic band-gap (EBG) structures: A low mutual coupling design for array applications," *IEEE Trans. Antennas Propag.*, vol. 51, no. 10, pp. 2936-2946, Oct. 2003.

[23] K. Yu, Y. Li, and X. Liu, "Mutual coupling reduction of a MIMO antenna array using 3-D novel meta-material structures," *Applied Computational Electromagnetics Society (ACES) Journal*, vol. 33, no. 7, pp. 758-763, Mar. 2018.

[24] A. Diallo, C. Luxey, P. L. Thuc, R. Staraj, and G. Kossiavas, "Study and reduction of the mutual coupling between two mobile phone pifas operating in the DCS1800 and UMTS bands," *IEEE Trans. Antennas Propag.*, vol. 54, no. 11, pp. 3063-3074, Nov. 2006.

[25] S. Luo, Y. Li, Y. Xia, and L. Zhang, "A low mutual coupling antenna array with gain enhancement using metamaterial loading and neutralization line structure," *Applied Computational Electromagnetics Society (ACES) Journal*, vol. 34, no. 3, pp. 411-418, Mar. 2019.

[26] W. Shi, X. Liu, and Y. Li, "ULA fitting for MIMO radar," *IEEE Commun Lett.*, vol. 26, no. 9, pp. 2190-2194, Sep. 2022.

[27] C. Wu, C. Chiu, and T. Ma, "Very compact fully lumped decoupling network for a coupled two-element array," *IEEE Antennas Wireless Propag. Lett.*, vol. 15, pp. 158-161, 2016.

[28] R. Xia, S. Qu, P. Li, D. Yang, S. Yang, and Z. Nie, "Wide-angle scanning phased array using an efficient decoupling network," *IEEE Trans. Antennas Propag.*, vol. 63, no. 11, pp. 5161-5165, Nov. 2015.

[29] X. Zou, G. Wang, Y. Wang, and H. Li, "An efficient decoupling network between feeding points for multielement linear arrays," *IEEE Trans. Antennas Propag.*, vol. 67, no. 5, pp. 3101-3108, May 2019.

[30] Y. Zhang, Q. Ye, G. F. Pedersen, and S. Zhang, "A simple decoupling network with filtering response for patch antenna arrays," *IEEE Trans. Antennas Propag.*, vol. 69, no. 11, pp. 7427-7439, Nov. 2021.

[31] Y.-M. Zhang and S. Zhang, "A novel aperture-loaded decoupling concept for patch antenna arrays" *IEEE Trans. Microw. Theory Techn.*, vol. 69, no. 9, Sep. 2021.

[32] C. Mao, S. Gao, Y. Wang, and J. T. S. Sumantyo, "Compact broadband dual-sense circularly polarized microstrip antenna/array with enhanced isolation," *IEEE Trans. Antennas Propag.*, vol. 65, no. 12, pp. 7073-7082, Dec. 2017.

[33] B. Liu, X. Chen, J. Tang, A. Zhang, and A. A. Kishk, "Co- and cross-polarization decoupling structure with polarization rotation property between linearly polarized dipole antennas with application to decoupling of circularly polarized antennas," *IEEE Trans. Antennas Propag.*, vol. 70, no. 1, pp. 702-707, Jan. 2022.

[34] D. Gao, Z. Cao, S. Fu, X. Quan, and P. Chen, "A novel slot-array defected ground structure for decoupling microstrip antenna array," *IEEE Trans. Antennas Propag.*, vol. 68, no. 10, pp. 7027-7038, Oct. 2020.

Xin Cheng received his Bachelor's degree in Optical Information Science and Technology from Shaanxi University of Science & Technology, Xi'an, China, in 2016. He is currently pursuing a Ph.D. degree in Electronic Science and Technology with Xi'an Jiaotong University, Xi'an, China. His current research interests include antenna array decoupling techniques and gap waveguide technology.

Bingyi Qian received his B.S. degree in Electronics and Information Engineering from Xidian University, Xi'an, China, in 2020, where he is currently pursuing an M.S. degree in Electronics Science and Technology from Xi'an Jiaotong University, Xi'an. His current research interests include microstrip antenna design, mutual coupling reduction, and 5G mobile antennas.

Le Chang received his B.S. degree in Electronics and Information Engineering from Xidian University, Xi'an, China, in 2012, and his Ph.D. degree in Electrical Engineering from Tsinghua University, Beijing, China, in 2017. From 2017 to 2020, he was with the Antenna and RF Group, Huawei Device Ltd., Beijing, where he worked as a Senior Engineer. Since 2021, he has been a Special Appointed Researcher with Xi'an Jiaotong University, Xi'an. His current research interests include 5G mobile antennas, millimeter-wave antennas, and phased arrays.

Jinlin Liu received his B.Sc. degree in communications engineering from the University of Electronic Science and Technology of China, Chengdu, China, in 2005. He received the Vordiploma degree from the Munich University of Technology, Munich, Germany, in 2011, and the Swedish Licentiate degree and Ph.D. degree from the Chalmers University of Technology, Gothenburg, Sweden, in 2016 and 2019, respectively. From 2005 to 2007, he was with Intel, Chengdu branch, as a Test Engineer. From 2013 to 2014, he was with Eurodesign GmbH, Munich, as a PCB Test Engineer. His current research interests include fundamental electromagnetic theory, millimeter-wave planar antennas in general, gap waveguide technology, and frequency-selective surfaces. He received the Best Student Paper Award First Place at the 2017 International Symposium on Antennas and Propagation. He serves on the Review Board for several journals, including the *IEEE Transactions on Antennas and Propagation*, the *IEEE Transactions on Microwave Theory and Techniques*, the *IEEE Transactions on Components, Packaging, and Manufacturing*, the *IEEE Antennas and Wireless Propagation Letters*, the *IEEE Microwave and Wireless Components Letters*, and the *Journal of Electromagnetic Waves and Applications*.

Xiaoming Chen received his B.Sc. degree in electrical engineering from Northwestern Polytechnical University, Xi'an, China, in 2006, and his M.Sc. and Ph.D. degrees in electrical engineering from the Chalmers University of Technology, Gothenburg, Sweden, in 2007 and 2012, respectively. From 2013 to 2014, he was a Post-Doctoral Researcher with the Chalmers University of Technology. From 2014 to 2017, he was with Qamcom Research and Technology AB, Gothenburg, Sweden. Since 2017, he has been a Professor at Xi'an Jiaotong University, Xi'an. His current research interests include multi-in multi-out (MIMO) antennas, over-the-air (OTA) testing, reverberation chambers, and hardware impairments and mitigation. Prof. Chen serves as a Senior Associate Editor (AE) for *IEEE Antennas and Wireless Propagation Letters*. He received the Outstanding AE Award in 2018, 2019, 2020, 2021, and 2022. He received the URSI (International Union of Radio Science) Young Scientist Award in 2017 and 2018.